Eur. Phys. J. D **10**, 19–26 (2000)

THE EUROPEAN PHYSICAL JOURNAL D

EDP Sciences

Lifetimes and transition probabilities of Xe II: Experimental measurements and theoretical calculations

H.O. Di Rocco[a], D.I. Iriarte, and J.A. Pomarico

Instituto de Física Arroyo Seco, Facultad de Ciencias Exactas, UNCPBA, Pinto 399, 7000 Tandil, Buenos Aires, Argentina

Received 15 July 1999

Abstract. In this work we make an experimental and theoretical investigation of transition probabilities (A) and lifetimes (τ) of Xe II. Eighteen A_{ij}'s corresponding to the $6p$–$6d$ array were measured using a Laser Produced Plasma (LPP) as the spectroscopic source. The *ab initio* (AI) and Least Square Fitting (LSF) approaches were used to calculate the atomic parameters. Relativistic corrections and Configuration Interaction (CI) effects have been taken into account using the HFR approach described by Cowan. Whereas the AI parameters corresponding to $6p$ levels are not very affected by CI effects, several of the $6d$ levels with $J = 1/2$, $3/2$ and $5/2$ making transitions to the fundamental levels $5p^5\ ^2\mathrm{P}_{1/2,3/2}$ are affected by CI effects due to both, discrete nd and continuum ϵd states, modifying their lifetimes values. An extensive comparison with other measurements and calculations are made. In particular, concerned with branching ratio and forbidden transitions.

PACS. 32.70.Cs Oscillator strengths, lifetimes, transition moments

1 Introduction

Singly ionized xenon (Xe II) provides an important case to test the validity of the *ab initio* (AI) method to calculate transition probabilities (A_{ij}) and lifetimes (τ_i) for complex ions. Xe II is a very well studied spectra [1] such that also the Least Squares Fit (LSF) method can be applied to the calculation of those atomic parameters. Then, both methods can be compared and therefore it is hoped that we can obtain conclusions to be applied to ions where the experimental information is scarce or inexistent to apply the LSF method. Applications in collision physics, photoelectronic, spectroscopy, plasma diagnostics, etc. require reliable data on A_{ij}'s and τ_i's of rare gas ions. From the analysis of the published data about Xe II, a showy discrepancy arises between the values provided by different authors, as well in the experimental as in the theoretical side.

The scope of this paper is multiple, and is in part an attempt to throw some light upon the origin of these discrepancies. On one hand, we have measured, in emission, the A_{ij}'s for eighteen lines corresponding to the $6p$–$6d$ array using a laser produced plasma (LPP) carefully tested [2]. This plasma is well described by a partial Local Thermodynamic Equilibrium (pLTE) model [3] during the firsts 20 ns after the laser pulse arrives. The relative intensities of $(6s + 5d)$–$6p$ and $6p$–$6d$ lines were measured at several instants of the pulse plasma during these 20 ns at intervals of the order of 2 ns. From these relative intensities and a provisional set of estimated or measured A_{ij}'s we obtain, simultaneously, the plasma temperature and the transition probabilities. In order to control the self-absorption, the relative intensities of three lines arising from the same upper level were studied, in accordance with the method explained in [4].

Our A_{6p-6d} values are compared both with the LSF and AI methods as it will be exposed in Section 5 below. The same set of calculations are used to compare experimental measurements of A_{5d-6p}'s and A_{6s-6p}'s and lifetimes of levels corresponding to the $6p$ and $6d$ configurations as well as other atomic parameters. This will be also explained in Section 5. We base our treatment on the Configuration Interaction method described by Cowan [5]. Although there are diverse theoretical options in atomic calculations, the validity of Cowan's methods even for atoms as heavy as lead ($Z = 82$) was stressed in a serie of papers by Biémont and Quinet [6]. Special care was taken with the line classification and level designations of all the analyzed papers; all results are given following the denominations by Hansen and Persson.

Anticipating the results we can say that the use of the LSF approach can need the re-scaling of the dipole integrals. The introduction of the continuum states can be of importance in the calculation of branching ratio as well as the lifetimes of some levels.

2 Experimental information

A revised and extended analysis of the spectrum of Xe II was made by Hansen and Persson [1], where 60 odd and

[a] e-mail: hdirocco@ifas.exa.unicen.edu.ar

101 even energy levels were identified on the basis of classifying 950 lines. Radiative lifetimes for Xe II have appeared in the literature at least since 1969 and several papers were published from that time on. However, we shall restrict our considerations principally to the newer works, published after 1980. Older works are properly cited in the references given at the end of this paper. The lifetime of the level $6p\ ^4\mathrm{P}_{5/2}$ was measured by Silverans *et al.* [7] using the fast-beam laser method. Their value was compared with three references previous to the 80's. The τ's of 15 levels belonging to the $6p, 6d$ and $7s$ configurations were measured by a delayed coincidence method by Fonseca *et al.* [8]; their values were compared with six experimental and two theoretical works. The τ's for eighteen levels of configurations $6d, 6d'$ and $7s$ were published by Blagoev *et al.* [9] These values are particularly interesting for our present work because several lifetimes are in strong disagreement with other values to be mentioned below.

Using the beam-laser method, Ward *et al.* [10] measured the τ's of three $6p$ levels; an erratum was published after the work of Bröstrom *et al.* [11] to be commented below. The values for seven levels belonging to $5p^4\ 6d$ configuration have been measured by Das and Bhattacharya [12]; one of the measurements are in strong disagreement with the value of Blagoev *et al.* The $\tau(6p\ ^4\mathrm{P}_{5/2})$ was measured by Mitchell *et al.* [13] using the cascade-photon-coincidence technique. Of particular interest is the work of Jullien *et al.* [14] because that authors measured the transition probabilities of electric dipole-forbidden transition $^2\mathrm{P}_{1/2} \rightarrow\ ^2\mathrm{P}_{3/2}$ and the corresponding $\tau(^2\mathrm{P}_{1/2})$. The A's for eighteen lines belonging to the $5d$–$6p$, $6s$–$6p$ and $6p$–$6d$ arrays were published by Gigosos *et al.* [15]; that values are compared with several sources, specially with the extensive measurements from Miller *et al.* [16]. The last work on $\tau(6p)$ levels was published by Bröstrom *et al.* with a beam-laser method. As in the works of Silverans *et al.* and Ward *et al.* cited above, the method is expected to be very accurate (because it do not suffer of cascade problems) and appears as a useful test for the theory. In the conclusions of their paper, and taking into account the calculations of Hansen and Persson and Garpman and Spector [17], Bröstrom *et al.* indicate that "theoretical efforts have not been able to provide values in close agreement with experiment". Our work is, in part, an attempt to give an answer to this discrepancy. On the other hand, the lifetime for the $5s5p^6\ ^2\mathrm{S}_{1/2}$ was measured very recently by Lauer *et al.* [18] using synchrotron radiation; also theoretical calculations using a CI method were carried out. Their value and the one by Rosenberg *et al.* [19] correspond between them within the limit of twice the quoted experimental uncertainties.

3 Experimental work and measurements

3.1 Experimental arrangement and plasma condition

Figure 1 schematically displays the main features of the experiment. We have employed a Nd:YAG laser (pulse width 7 ns, 650 mJ @ 10 Hz) emitting in the 1.06 μm line. The laser beam was focused onto a cell with spectroscopically pure Xe by means of a antireflection coated quartz lens of 20 cm focal length. The cell consisted of a pyrex glass tube with two windows at the ends and a third window at right angle with the tube axis, forming a T. The light emitted from the plasma was gathered by another quartz lens of 20 cm focal length and then analyzed by a monochromator having a resolution of 300 000 and equipped with a photomultiplier (PM).

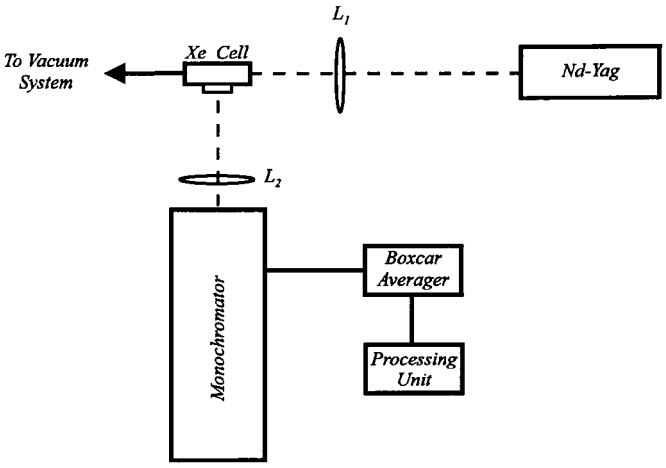

Fig. 1. Experimental setup.

The signal produced by the PM is then analyzed by a Box-Car integrator with gate widths between 1 and 10 ns, connected to a PC where data is acquired. The signal processing was made by normal statistical-fitting software.

The energy of the laser pulse was measured by means of a volume Scientech calorimeter, model MC2501. This measurement device could be used in front of the cell intercepting the beam, or behind the second end window to estimate the energy content of the beam after the plasma has been formed.

We worked at about 300 torr filling pressure and with laser energies of about 400 mJ. Under this conditions, a small ball – like plasma is obtained which is very stable in its position with respect to the spectral analysis system. By placing a suitable diaphragm in order to gather only the light coming from the periphery of the plasma, it can be concluded that the ions observed are the same as those when detecting all the light (without any diaphragm). Moreover, the times of appearance of each ion are unchanged within experimental error (for the checking purpose the gate width of 1 ns was used).

A time and frequency detailed analysis was done on the Xe plasma. As it was shown in reference [2] the central portion of the plasma shows a second peak in emission at later times due to a radiative recombination process, while in the periphery all transitions consist of a single peak. Moreover, in the studied interval (10 to 30 ns after laser firing), the experimental conditions for LTE were verified. From the measurements of linewidths and the ratio between line intensities, an electron density of 3×10^{16} cm^{-3} and an electron temperature between 1.5 and

1.8 eV was found in such interval. The width of the exit slit in front of the PM was set to 300 μm, in order to measure the relative integrated intensities of the lines. The intensities were measured during 20 ns at intervals of 2 ns, in order to calculate the electron temperature as a function of the time and as a part of the process to measure the relative transition probabilities.

3.2 Considerations about self-absorption

In a previous work from Bertuccelli *et al.* [4] two important types of corrections in detailed line measurements were considered: (i) the level populations which differ from those in thermal equilibrium and (ii) the importance of optical depth effects. In our LPP, levels are populated by collisions with electrons and depopulated by radiative and collisional processes. A schematic two-level system including collisional excitation $i \rightarrow k$ (measured by the rate C_{ik}) and de-excitation $k \rightarrow i$ (measured by the rate C_{ki}) plus the radiative decay of the upper level given by A_k was considered. From the balance equation the ratio between the level populations is given by:

$$\frac{N_k}{N_i} = \frac{(N_k/N_i)_{\rm eq}}{1+\alpha_{ki}}, \qquad (1)$$

where the parameter $\alpha_{ki} = A_k/C_{ki}$ describes the deviation from the LTE limit. The main temperature dependence is given by the Boltzmann factor $\exp(-\Delta E/kT)$, the same as in the equilibrium case. Using a semi-quantitative approach to calculate collisional rates, it results that the dependence of α_{ki} with T and N is given by $\alpha_{ki} \propto T^{1/2}N^{-1}$. With respect to the criterium for the validity of the pLTE state, it was concluded that the experimental conditions are suitable for measuring intensity ratios within a pLTE model. Concerning with the source thickness, the analysis of two (or better three) lines arising from the same upper level is a good test to check the absence of self-absorption; a constant relation between their intensities provides that check. As it is known, the consequence of a non negligible thickness is that the line of greater A_{ij} decreases it relative intensity as compared with other lines arising from the same level (see the experimental measurements reported in Ref. [4]). In Figure 2 the temporal behavior of the lines of 4245, 4585 and 4545 Å arising from the level 135 507 cm^{-1} are shown, whereas in Figure 3 the ratio between the lines 4245 Å and 4585 Å is observed. From this Figure, we can see that, between 7 and 27 ns after laser pulse peak, the ratio remains almost constant about the mean value 1.20 ± 0.15. Therefore we conclude that in that range the source can be considered to be optically thin.

3.3 Determination of the excitation temperature and transition probabilities

To compute atomic transition probabilities (A_{ij}) we propose an algorithm starting from the intensity data of a set of spectral lines corresponding to a given ion. The available intensity data may be either the integrated line profile of each line or a temporal register $I(t)$. A set of initial A_{ij}'s values, available either from previous results or theoretical calculations, is supposed to be known. Besides, the multiplicity and energy of the involved levels as well as the wavelengths of the measured lines must be included in the input data.

The basic idea is to use the information contained in all measured lines to improve the calculation of each A_{ij}.

Every iteration of the algorithm goes through the following steps.

1. By selecting a convenient reference line and using the initial values for the A_{ij}'s, the corresponding temperatures for each line are calculated accordingly to the

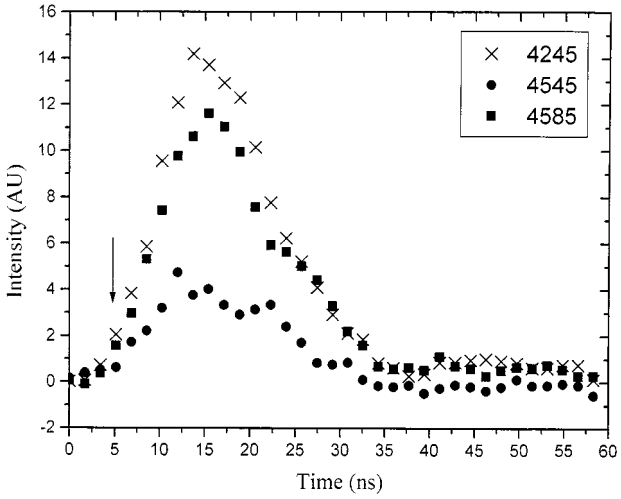

Fig. 2. Temporal behavior of the lines of 4245, 4585 and 4545 Å. The arrow shows the time of the laser pulse peak.

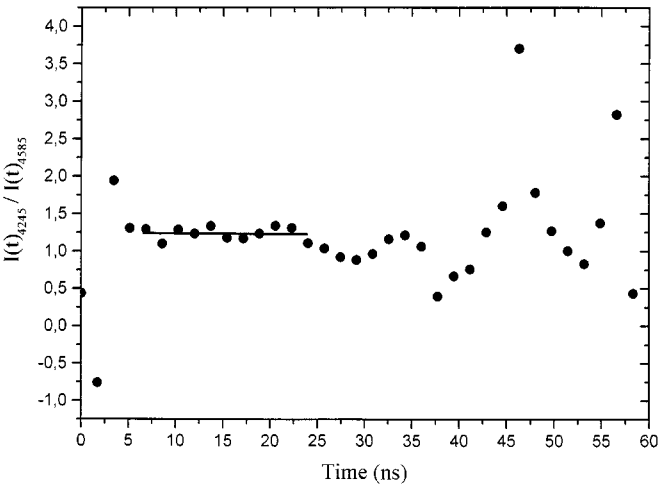

Fig. 3. Ratio between lines 4245 and 4585 Å as a function of time. The segment shows the almost constant ratio interval between 7 and 27 ns after the laser pulse peak.

elementary formula:

$$kT = \frac{\Delta E}{\ln Y}, \tag{2}$$

where ΔE is the energy gap between the line upper level and the reference line upper level. The term Y is obtained from:

$$Y = \frac{g_l A_{lj} \omega_{lj} I_{ki}}{g_k A_{ki} \omega_{ki} I_{lj}}, \tag{3}$$

being $k \to i$ the measured line transition and $l \to j$ the reference line transition, where I denotes intensity, ω represents the angular frequency of the transition and g is the level multiplicity.
This can be seen as a two points Boltzmann plot, one of them (the corresponding to the reference line) being at the origin of coordinates.

2. For each temperature, the A_{ij}'s can be re-evaluated together with the resulting standard deviation for the present iteration
3. The vector containing the initial A_{ij}'s is overwritten with these new values and the process begin again until a desired convergence degree is reached.

As in every Boltzmann-plot, care must be taken so that the energy difference between the line and the reference line is large enough such as to minimize errors in evaluating the temperature.

In case that a temporal record of the lines intensities, $I(t)$, is available (as in our case) the first step is repeated for each time (or for a set of times where both, a good signal to noise ratio holds and the spectroscopic source can be considered to be optically thin). As a result the temperature is obtained as a function of time, $T(t)$. Since A_{ij} must be independent of time, this allows to calculate each of them as described in step 2 for each time and to average these values in order to obtain the new A_{ij}.

Moreover, the A_{ij}'s must also be insensitive to the chosen reference line. Thus the whole procedure may be repeated for a given number of reference lines for obtaining a new average value of each transition probability.

4 Calculations

In this work both the AI and LSF approaches to the configuration interaction method are used. Relativistic Hartree-Fock orbitals are employed as base functions in the former case. The atomic parameters to be considered are: (i) transition probabilities for the $(5d + 6s)$–$6p$ and $6p$–$6d$ arrays, (ii) lifetimes for the $5s5p^6, 6p$ and $6d$ levels, (iii) the electric dipole-forbidden transition $^2\mathrm{P}_{1/2} \to {}^2\mathrm{P}_{3/2}$ and the corresponding lifetime $\tau(^2\mathrm{P}_{1/2})$ and (iv) the branching ratio for the transitions $5s5p^6\ {}^2\mathrm{S}_{1/2}$ to the $5s^25p^5\ {}^2\mathrm{P}_{1/2,3/2}$ levels, which resulted very sensitive to the eigenvector composition.

4.1 LSF Values for A_{ij}'s and τ's

It is believed that the consideration of the LSF procedure does improve not only the calculated positions of the levels but generally also the calculated A_{ij}'s and the corresponding τ's. Hansen and Persson [1] found that a single configuration LSF provides a precise description of the $6p$ configuration; the mean error of the fit is 55 cm^{-1}. However, for even configurations it is difficult to obtain an adequate fit because many upper levels remain unknown; moreover, the number of parameters is large. The configurations

$$5s5p^6, \text{ and } 5s^25p^4(6s + 7s + 8s + 5d + 6d + 7d)$$

have been treated together and the LSF procedure yields in many cases discrepancies up to 700 cm^{-1}. Using the LSF values from Hansen and Persson, the four types of atomic parameters above mentioned were calculated. The lifetimes of the $6p$ levels and the branching ratio are given in this reference and they are presented here for completeness. As will be explained in greater detail in Section 5, the transition probabilities for the $(5d + 6s)$–$6p$ and $6p$–$6d$ arrays, when compared with the new measurements of Gigosos *et al.* [15], shows a very good correlation. On the other hand, the comparison between LSF and experimental values of the τ_{6p}'s is interesting and deserves a greater discussion which will be postponed to Section 5. As noted in reference [1], the calculated branching ratio for the transitions $5s5p^6$ to the $5s^25p^5\ {}^2\mathrm{P}_{1/2,3/2}$ is far from being satisfactory (see Sect. 5).

4.2 Ab initio calculations

Electron-electron correlations and approximate relativistic effects have been taken into account using the configuration interaction plus relativistic Hartree-Fock technique due to Cowan [5]. This approach allows the study of correlation effects through the CI method considering the different types of correlation as classified by Sinanoglu *et al.*: internal, semi-internal and all-external [20]. The relativistic effects are introduced by considering a Pauli-type approximation to the Dirac H-F equations. Core polarization effects ($4d$ core) have been introduced in the model by opening the $4d$ shell, but this does not produce noticeable effects. On the other hand, part of the polarization effects is taken implicitly into account by scaling down the Slater integrals. Autoionization configurations were also considered, which can affect the magnetic dipole ($M1$) and electric quadrupole ($E2$) transition probabilities of the ground configurations in about 5% but produces negligible effects on the $6p$ levels.

Several runs were made for diverse calculations of AI Slater parameters. It is known empirically that the computed energy-level intervals agree better with experiment if the Coulomb parameters are smaller than theoretical. The typical values 0.80, 1.00, 0.90, 0.90 and 0.90 were taken in all cases as scaling factors for the radial parameters $F^2(5p, 5p)$, ξ, $F^2(5p, nl)$, $G^k(5p, nl)$ and $R^k(ij, tu)$

Table 1. Weighted transition probabilities in units of 10^8 s^{-1} of $6p \rightarrow (5d + 6s)$ array.

λ (Å)	LS designation	HPLS	HPAI	AIMC	AIWC	[15]
4603.03	$6s^2\mathrm{P}_{3/2}$–$6p^2\mathrm{P}_{3/2}$	3.87	1.96	1.83	2.35	3.01
4844.33	$6s^4\mathrm{P}_{5/2}$–$6p^4\mathrm{D}_{7/2}$	9.96	8.71	8.68	8.55	6.94
4883.53	$6s^4\mathrm{P}_{1/2}$–$6p^4\mathrm{D}_{3/2}$	2.88	2.95	2.96	3.04	2.68
4887.30	$6s^4\mathrm{P}_{3/2}$–$6p^4\mathrm{S}_{3/2}$	1.06	1.54	1.36	1.36	1.07
4988.77	$5d^2\mathrm{P}_{1/2}$–$6p^2\mathrm{D}_{3/2}$	0.89	0.94	0.84	0.83	0.84
5292.22	$6s^4\mathrm{P}_{5/2}$–$6p^4\mathrm{P}_{5/2}$	6.86	7.00	7.00	7.14	5.42
5309.27	$6s^4\mathrm{P}_{3/2}$–$6p^4\mathrm{D}_{3/2}$	0.74	0.71	0.74	0.75	0.89
5339.33	$6s^4\mathrm{P}_{5/2}$–$6p^4\mathrm{P}_{3/2}$	2.81	2.48	2.41	2.33	2.67
5419.15	$6s^2\mathrm{P}_{3/2}$–$6p^2\mathrm{D}_{5/2}$	5.44	2.78	2.94	3.75	3.89
5438.96	$6s^4\mathrm{P}_{3/2}$–$6p^4\mathrm{P}_{1/2}$	1.69	1.86	1.86	1.85	1.71
5460.39	$5d^4\mathrm{D}_{5/2}$–$6p^4\mathrm{D}_{7/2}$	0.64	0.95	0.98	1.17	0.51
6051.15	$5d^4\mathrm{D}_{7/2}$–$6p^4\mathrm{P}_{5/2}$	1.28	1.51	1.48	1.49	1.23

respectively; no other scaled or fitted value were used. It is important to note that the conclusions of this work are not dependent on the scaling factors nor on the inclusion of the Trees' correction $\alpha L(L+1)$; the α parameter was not used in the obtention of the present results. For brevity, radial parameters used in the calculations are not presented here.

4.2.1 Restricted set of configurations

In order to test the generally accepted hypothesis that LSF values for A_{ij}'s and τ's should be better than the AI ones, the same configurations considered by Hansen-Persson were used: the odd $6p$ and the even $5s5p^6$, and $5s^25p^4(6s + 7s + 8s + 5d + 6d + 7d)$ configurations.

Briefly, the average values for the A_{ij}'s are very similar to LSF ones; however, the τ_{6p} values are clearly in better accordance with the experiment.

4.2.2 Extended set of configurations and introduction of continuum states

In this case we first used the odd

$$5s^25p^5 + 5s^2\ 5p^4(np + mf);\ n = 6\text{–}10,\ m = 4\text{–}8$$

and the even

$$5s5p^6 + 5s^25p^4(qs + rd);\ q = 6\text{–}9,\ r = 5\text{–}12$$

configurations. This is an obvious approach used in many papers treating about line classifications and levels calculations. Moreover, also the continuum ϵd states ($\epsilon = 0 - 64Ry$) were introduced in addition to the above bound ones. This approach was used also by Lauer *et al.* [18] in their recent paper about the lifetime of the $5s5p^6$ level.

In average, the comparison with measured transition probabilities indicates that all values are in similar agreement. With respect to the lifetimes, the introduction of the extended set improves the accordance with the experimental values. As will be shown in Section 5, the introduction of the continuum states is very important in the calculation of the branching ratio, as well as in the lifetime of the $5s5p^6\ {}^2\mathrm{S}_{1/2}$ level.

5 Results and tables

In Table 1 we show the transition probabilities of the $(5d + 6s)$–$6p$ arrays multiplied by the respective $2J + 1$ value of the upper levels for twelve lines. After the columns indicating the wavelengths and LS classifications, there are our four set of calculations and in the last column the experimental values of Gigosos. HPLS indicates the values obtained with the LSF parameters from the paper of Hansen and Persson. HPAI indicates that the same set of configurations of [1] is used in the *ab initio* form. AIMC signifies that we used the extended set of bound configurations whereas AIWC indicates the inclusion of the continuum states. Making the ratio between theoretical and experimental results, the mean and standard deviations are, respectively: HPLS/exp $= 1.05 \pm 0.31$, HPAI/exp $= 1.03 \pm 0.38$, AIMC/exp $= 1.01 \pm 0.38$ and AIWC/exp $= 1.05 \pm 0.46$.

Table 2 is in all aspects similar to the Table 1 but using our measurements for eighteen $6p$–$6d$ transitions. To our knowledge, they have not been previously measured. The corresponding mean and standard deviations are, respectively: HPLS/exp $= 0.94 \pm 0.32$, HPAI/exp $= 0.97 \pm 0.39$, AIMC/exp $= 0.96 \pm 0.24$ and AIWC/exp $= 0.97 \pm 0.25$.

Table 3 shows the comparison between calculated and experimental lifetimes of the $6p$ levels. The respective experimental results to be compared are from the works of Fonseca *et al.*, Silverans *et al.*, Ward *et al.*, Mitchell *et al.* and Bröstrom *et al.* cited above. We can see that the values from the last four authors (in all cases using the beam-laser method) are very similar, whereas the values of Fonseca *et al.* (that used the delayed coincidence method) are greater. Despite the fact that the LSF values are systematically 2 ns lower than experimental ones, there exists a very good correlation between both sets. The LSF values for the τ_{6p} indicates that, with respect to the experimental values of the last cited authors, $\tau_{\mathrm{exp}}/\tau_{\mathrm{LSP}} = 1.21 \pm 0.03$.

Table 2. Weighted transition probabilities in units of 10^8 s^{-1} of $6d \rightarrow 6p$ array.

λ (Å)	LS designation	HPLS	HPAI	AIMC	AIWC	Exp
3907.91	$6p^2\mathrm{D}_{5/2}$–$6d^2\mathrm{D}_{5/2}$	3.03	2.53	2.42	2.63	2.33
4158.04	$6p^4\mathrm{P}_{1/2}$–$6d^4\mathrm{D}_{1/2}$	3.95	3.93	3.72	3.78	2.88
4180.10	$6p^4\mathrm{P}_{3/2}$–$6d^4\mathrm{D}_{3/2}$	6.06	6.59	6.25	6.29	5.00
4193.15	$6p^2\mathrm{F}_{5/2}$–$6d^2\mathrm{G}_{7/2}$	18.0	18.2	17.8	17.9	17.28
4208.48	$6p^4\mathrm{P}_{3/2}$–$6d^4\mathrm{D}_{5/2}$	5.02	5.46	5.12	5.21	4.58
4223.00	$6p^4\mathrm{S}_{3/2}$–$6d^2\mathrm{F}_{5/2}$	3.87	4.20	6.13	6.44	7.43
4238.25	$6p^4\mathrm{P}_{5/2}$–$6d^4\mathrm{D}_{5/2}$	7.28	7.89	7.51	7.63	6.67
4245.38	$6p^4\mathrm{P}_{5/2}$–$6d^4\mathrm{D}_{7/2}$	12.0	12.1	10.9	11.0	8.51
4330.52	$6p^2\mathrm{D}_{5/2}$–$6d^2\mathrm{F}_{7/2}$	16.0	15.7	15.8	15.8	11.72
4393.20	$6p^4\mathrm{D}_{3/2}$–$6d^4\mathrm{F}_{5/2}$	11.5	12.0	11.6	11.5	13.00
4395.77	$6p'^2\mathrm{F}_{7/2}$–$6d'^2\mathrm{G}_{9/2}$	22.7	22.4	21.7	21.8	24.72
4448.13	$6p^4\mathrm{D}_{5/2}$–$6d^4\mathrm{F}_{7/2}$	17.1	17.3	16.8	16.8	21.21
4462.19	$6p^4\mathrm{D}_{7/2}$–$6d^4\mathrm{F}_{9/2}$	21.8	21.9	21.2	21.3	23.94
4480.86	$6p^2\mathrm{P}_{3/2}$–$6d^2\mathrm{D}_{5/2}$	4.43	4.31	5.50	5.69	6.99
4540.89	$6p^2\mathrm{D}_{3/2}$–$6d^4\mathrm{P}_{5/2}$	3.98	7.10	7.30	6.65	10.37
4545.23	$6p^2\mathrm{D}_{5/2}$–$6d^4\mathrm{D}_{7/2}$	1.46	1.44	1.37	1.41	2.98
4577.06	$6p^4\mathrm{D}_{7/2}$–$6d^4\mathrm{D}_{5/2}$	1.03	1.21	1.12	1.14	1.41
4585.48	$6p^4\mathrm{D}_{7/2}$–$6d^4\mathrm{D}_{7/2}$	5.87	5.71	5.76	5.80	7.61

Table 3. Comparison between calculated and experimental lifetimes (τ) of the $5s^25p^46p$ levels of Xe II.

J	Level	Designation	HPLS	HPAI	AIMC	[8]	[7]	[10]	[13]	[11]
7/2	130 064	$(^1\mathrm{D})^2\mathrm{F}$	5.56	6.25	6.24	8.2 ± 0.5				7.3 ± 0.2
	113 705	$(^3\mathrm{P})^4\mathrm{D}$	4.97	6.08	6.09	8.0 ± 0.8		6.9 ± 0.2		6.8 ± 0.2
5/2	132 208	$(^1\mathrm{D})^2\mathrm{D}$	6.13	6.84	6.86					
	128 867	$(^1\mathrm{D})^2\mathrm{F}$	6.99	7.38	7.16					
	123 113	$(^3\mathrm{P})^4\mathrm{D}$	5.20	6.17	6.14	7.5 ± 0.5		7.3 ± 0.2		7.2 ± 0.2
	113 512	$(^3\mathrm{P})^2\mathrm{D}$	7.01	8.52	8.58				9.5 ± 0.1	9.3 ± 0.2
	111 959	$(^3\mathrm{P})^4\mathrm{P}$	5.57	6.49	6.51		7.5 ± 0.2	7.9 ± 0.2		7.8 ± 0.2
3/2	149 192	$(^1\mathrm{S})^2\mathrm{P}$	5.79	6.14	5.48					
	131 924	$(^1\mathrm{D})^2\mathrm{D}$	6.68	7.11	7.12	9.0 ± 0.5				
	129 667	$(^1\mathrm{D})^2\mathrm{P}$	4.86	5.04	5.47	7.7 ± 0.6				
	124 289	$(^3\mathrm{P})^2\mathrm{D}$	6.36	7.46	7.43	9.0 ± 0.9				
	123 255	$(^3\mathrm{P})^4\mathrm{S}$	6.76	7.23	7.45					
	121 629	$(^3\mathrm{P})^4\mathrm{D}$	5.52	6.37	6.29					
	116 783	$(^3\mathrm{P})^2\mathrm{P}$	5.94	7.03	7.31	9.2 ± 0.5				
	111 792	$(^3\mathrm{P})^4\mathrm{P}$	6.25	7.13	7.18	8.5 ± 0.8				
1/2	148 225	$(^1\mathrm{S})^2\mathrm{P}$	6.62	6.58	7.36					
	132 741	$(^1\mathrm{D})^2\mathrm{P}$	4.49	4.81	5.33	7.8 ± 0.8				
	124 571	$(^3\mathrm{P})^2\mathrm{S}$	6.94	7.41	7.51	8.6 ± 0.8				
	121 180	$(^3\mathrm{P})^4\mathrm{P}$	5.83	6.73	6.75					
	120 415	$(^3\mathrm{P})^4\mathrm{D}$	6.38	7.07	7.00					
	113 673	$(^3\mathrm{P})^2\mathrm{P}$	6.27	6.99	7.06					

This excellent correlation means, in our opinion, that in the LSF approach also the dipole integrals should be considered as adjustable parameters (in the present case the HFR integrals $\langle 6p/r/6s\rangle$ and $\langle 6p/r/5d\rangle$ should be divided by 1.1). It is important to remark that our results are not exactly those of Hansen and Persson because we used the relativistic version of the code for the calculation of wave functions and integrals. *Ab initio* values, using both the restricted and the extended set of bound configurations shows very similar results, and are systematically 1 ns over the LSF and 1 ns under the experimental ones.

The last table (Tab. 4) is similar to Table 3, but for the $6d$ levels. A column with the introduction of continuum configurations is added to the theoretical set. For the levels with $J = 9/2$ and $7/2$ all theoretical calculations are very similar. Great differences arises between the results

Table 4. Comparison between calculated and experimental lifetimes (τ) of the $5s^25p^46d$ levels of Xe II.

J	Level	Designation	HPLS	HPAI	AIMC	AIWC	[8]	[9]	[12]
9/2	136 109	$(^3P)^3P$	4.58	4.56	4.72	4.69			
	152 806	$(^1D)^1D$	4.41	4.47	4.60	4.57			
7/2	136 597	$(^3P)^2F$	4.44	4.58	4.54	4.54		6.3 ± 0.5	
	135 507	$(^3P)^4D$	4.12	4.16	4.43	4.39		6.6 ± 0.5	6.3 ± 0.4
	145 587	$(^3P)^4F$	4.59	4.55	4.70	4.68			
	152 708	$(^1D)^2G$	4.03	4.09	4.20	4.18			
	153 978	$(^1D)^2F$	5.21	5.15	5.34	5.39		7.2 ± 0.6	6.8 ± 0.4
5/2	139 094	$(^3P)^2D$	0.24	0.24	0.24	0.27		< 3	6.0 ± 0.4
	135 547	$(^3P)^4D$	4.24	3.90	4.16	4.11	5.1 ± 0.7	6.2 ± 0.6	4.6 ± 0.3
	146 927	$(^3P)^2F$	0.84	0.70	0.59	0.66			
	146 305	$(^3P)^4P$	1.33	3.89	3.56	3.24	4.5 ± 0.5		
	144 384	$(^3P)^4F$	2.73	2.71	2.86	2.95		4.7 ± 0.5	
	153 585	$(^1D)^2F$	4.85	4.07	1.28	1.67			
	154 032	$(^1D)^2D$	0.26	0.31	3.78	3.70		3.4 ± 0.4	
3/2	135 708	$(^3P)^4D$	2.10	3.32	3.63	3.53	5.0 ± 0.6	6.7 ± 0.6	6.5 ± 0.4
	139 640	$(^3P)^4P$	0.21	0.18	0.18	0.20			
	145 940	$(^3P)^2D$	1.03	0.91	0.96	1.17		3.5 ± 0.3	3.2 ± 0.2
	148 085	$(^3P)^2P$	0.36	0.53	0.46	0.37		< 3	
	144 140	$(^3P)^4F$	2.58	2.58	2.66	2.78		5.3 ± 0.5	8.1 ± 0.5
	154 608	$(^1D)^2D$	0.19	0.26	0.76	0.90			
	153 584	$(^1D)^2P$	0.31	0.34	0.26	0.50			
1/2	136 554	$(^3P)^2P$	0.44	1.58	1.33	0.25			
	138 726	$(^3P)^4P$	0.17	0.23	0.24	0.77			
	145 222	$(^3P)^4D$	1.47	1.19	1.36	1.68		4.5 ± 0.4	
	154 382	$(^1D)^2P$	0.16	0.58	1.40	0.66			

using the sets used by Hansen and Persson (both LSF and AI) and those using the extended sets for the levels with $J = 5/2$, 3/2 and 1/2, specially for those levels which have, in intermediate coupling, their higher purity as doublets and so are labeled in the LS scheme. It is important to note that the results are very weakly dependent on the scaling factors multiplying the radial parameters. When differences are remarkable, the introduction of the continua improves the agreement with the experiment.

With respect to experimental values there are discrepancies between the different authors. Of special importance is the analysis of the following levels: (1) 139 094 cm^{-1}, the value of Blagoev *et al.* is $\tau < 3$ ns, in very well accordance with the theoretical calculations, whereas Das and Bhattarchaya gives 6 ns. Because these authors have an equipment with a time resolution of nearly 3 ns, as indicated in a previous article about the levels of Ar II [21], they cannot measure very short lifetimes. Moreover, the line with a wavenumber of 139 094 cm^{-1} is observed in the VUV spectra [1] and because the transition probability depends on σ^3, that line determines basically the lifetime. (2) 146 305 cm^{-1}, the LSF value is very low whereas AI values are in near accordance with the measurements of Fonseca *et al.* (3) 153 585 cm^{-1}, the restricted set produce values greater than the extended set; because that line is present in VUV spectra [1], we think that the calculations with many configurations is more reliable, (4) 154 032 cm^{-1}, the use of many configurations produces a result in accordance with the experiment whereas the restricted set produces very low values, (5) 148 085 cm^{-1}, the low values obtained with all calculations are in accordance with the value of Blagoev *et al.* [9] (< 3 ns).

Concerning with the electric dipole-forbidden transition $^2P_{1/2}$–$^2P_{3/2}$ and the radiative lifetime of the $^2P_{1/2}$ state, the magnetic dipole (A_m) and the electric quadrupole (A_q) have been calculated by Garstang [22]. Their values are respectively 21 and 0.17 s^{-1} implying a lifetime of 47.2 ms. Using the monitor ion technique in a triple ICR spectrometer with Fourier transform detection Jullien *et al.* [14] measured a lifetime of 48.7 ± 5 ms. In our case, using only the p^5 configuration, the values are $A_m = 19.10$ s^{-1} and $A_q = 0.146$ s^{-1} producing a lifetime of 52 ms. The use of the set $5s^25p^5 + 5s^2\ 5p^4(np + mf)$; $n = 6$–10, $m = 4$–8 does not produce noticeable changes, due to the low interaction effects between np and mf states with the ground configuration.

With respect to the branching ratio for the transitions from $5s5p^6$ to $5s^25p^5$ levels, the LSF from Hansen and Persson is 0.148 that must be compared with the experimental value of 2. Hansen and Persson correctly indicates that the experimental values could be not very accurate. Indeed, in VUV spectra taken by one of us (HODR) and Dr. Persson at the University of Lund, the experimental

intensities were inconsistent with the measurements of Boyce, used by Hansen-Persson in their work about the spectrum of Xe II. Because of this, we indicates the theoretical values of the ratio $5s5p^6{-}^2\mathrm{P}_{3/2}/5s5p^6{-}^2\mathrm{P}_{1/2}$ for the different sets, only for showing the difficulties associated with these calculations. HPLS: 0.148 [1], HPAI: 10.164, AIMC: 42.31 and AIWC: 4.67.

The last calculations are referred to the lifetime of the $5s5p^6$ level. The experimental value of Rosenberg *et al.* is 34.4 ± 0.6 ns [19] whereas the new paper of Lauer *et al.* gives 35.9 ± 0.2 ns [18]. The LSF value obtained by Hansen and Persson is 32.1 ns; using the same set of configurations, the *ab initio* value resulted in 21 ns. Using many bound configurations, the value is 16 ns whereas the introduction of the continuum states, with $\epsilon = 0{-}64Ry$ produces 36 ns.

6 Conclusions

We measured for the first time eighteen transition probabilities corresponding to the $6p$-$6d$ array using temporal spectra from a laser produced plasma. Temperature and transition probabilities were derived from intensity measurements and a set of measured reference lines taken from the recent work of Gigosos *et al.* Diverse calculations were carried out in order to test the feasibility of the *ab initio* method when there are not sufficient experimental levels such us to use the least squares approach. Comparison with experimental data about transition probabilities and lifetimes indicates that using sufficient basis states and the configuration interaction schema, better values are obtained. This is specially true with respect to the lifetimes of the levels that make transitions to the fundamental ones, as well as in the calculation of branching ratio and, specially, with the lifetime of the $5s5p^6$ level.

In general, the agreement between the measured and calculated transition probabilities is good. With respect to the lifetimes of the $6p$ levels, the results taken with the beam-laser method are coherent between them and show a very good correlation with the calculations. Differences could be decreased scaling the transition integrals. With respect to the lifetimes of the $6d$ levels, theoretical values are systematically lower than experimental ones. However, calculations shows unambiguously that some values of Das and Bhattarchaya are inconsistent and better credits are given to the measurements of Blagoev *et al.*, specially with those doublet levels with lifetimes less than 3 ns.

A final, general comment must be made with respect to the designations of the levels and line classification. Several recent authors used older works and not the extensive research of Hansen and Persson, that is the most complete and accurate. Similarly, references to the calculations of Garpman and Spector, making single configuration calculations, must be rejected. Their results have to be interpreted as mere upper limits to the true lifetimes as they include only the $6p \rightarrow 6s$ (and not $6p \rightarrow 5d$) transitions in the lifetime determination.

Discussions with Dr. Fausto Bredicce, from the Centro de Investigaciones Opticas, La Plata, and the help of Dr. Graciela Bertuccelli with the experimental arrangement are gratefully acknowledged. Financial support from the CONICET, Agencia Nacional de Promoción Científica y Tecnológica and the Universidad Nacional del Centro are acknowledged.

References

1. J.E. Hansen, W. Persson, Phys. Scripta **36**, 602 (1987).
2. G. Bertuccelli, H.O. Di Rocco, D.I. Iriarte, M. Romeo y Bidegain, H.F. Ranea Sandoval, J. Quant. Spectrosc. Radiat. Transfer **61,** 309 (1999).
3. H.R. Griem, *Principles of Plasma Spectroscopy* (Cambridge Univ. Press, Cambridge, 1997).
4. G. Bertuccelli, H.O. Di Rocco, J. Quant. Spectrosc. Radiat. Transfer **55,** 463 (1996).
5. R.D. Cowan, *The Theory of Atomic Structure and Spectra* (University of California Press, Berkeley and Los Angeles, 1981).
6. E. Biémont, P. Quinet, Phys. Scripta **54**, 36 (1996) and references therein.
7. R.E. Silverans, G. Borghs, P. De Bisschop, M. van Hove, J.-M. van den Cruyce, J. Phys. B: At. Mol. Phys. **14**, L15 (1981).
8. V. Fonseca, M. Ortiz, J. Campos, J. Opt. Soc. Am. Lett. **73**, 1070 (1983).
9. K. Blagoev, N. Dimitrov, M. Drenska, J. Phys. B: At. Mol. Phys. **17**, 2189 (1984).
10. L. Ward, A. Wännström, A. Arnesen, R. Hallin, O. Vogel, Phys. Scripta **31**, 149 (1985).
11. L. Bromström, S. Mannervik, A. Passian, G. Sundström, Phys. Rev. A **49,** 3333 (1994).
12. M.B. Das, R. Bhattacharya, Phys. Scripta **44**, 145 (1991).
13. R.E. Mitchell, S.D. Rosner, T.J. Scholl, R.A. Holt, Phys. Rev. A **45**, 4452 (1992).
14. S. Jullien, J. Lemaire, S. Feinstein, M. Heninger, G. Mauclaire, R. Marx, Chem. Phys. Lett. **212**, 340 (1993).
15. M.A. Gigosos, S. Mar, C. Perez, I. de la Rosa, Phys. Rev. E **49**, 1575 (1994).
16. M.H. Miller, R.A. Roig, R.D. Bengtson, Phy. Rev. A **8**, 480 (1973).
17. S. Garpman, N. Spector, J. Opt. Soc. Am. **66**, 904 (1976).
18. S. Lauer *et al.*, J. Phys. B: At. Mol. Phys. **32**, 2015 (1999).
19. R.A. Rosenberg *et al.*, J. Phys. B: At. Mol. Phys. **11**, L719 (1978).
20. A. Hibbert, in *Computational Atomic Physics*, edited by K. Bartschat (Springer, Berlin, 1996).
21. M.B. Das, R. Bhattacharya, Z. Phys. D **14**, 25 (1989).
22. R.H. Garstang, J. Res. Nat. Bur. Stand. A **68**, 61 (1964).